Competition between magnetic field dependent band structure and coherent backscattering in multiwall carbon nanotubes

B. Stojetz, S. Roche†, C. Miko‡, F. Triozon†, L. Forró‡, C. Strunk

Institute of Experimental and Applied Physics, University of Regensburg, D-93040 Regensburg, Germany
†*Commissariat à l'Énergie Atomique, DRFMC/SPSMS, F-38054 Grenoble, France*
‡*Institute of Physics of Complex Matter, FBS Swiss Federal Institute of Technology (EPFL), CH-1015 Lausanne, Switzerland*
(Dated: 3 July 2006)

Magnetotransport measurements in large diameter multiwall carbon nanotubes (20-40 nm) demonstrate the competition of a magnetic-field dependent bandstructure and Altshuler-Aronov-Spivak oscillations. By means of an efficient capacitive coupling to a backgate electrode, the magnetoconductance oscillations are explored as a function of Fermi level shift. Changing the magnetic field orientation with respect to the tube axis and by ensemble averaging, allows to identify the contributions of different Aharonov-Bohm phases. The results are in qualitative agreement with numerical calculations of the band structure and the conductance.

The growing interest on molecular scale electronic transport has motivated much research on carbon nanotubes[1]. Single-wall carbon nanotubes with small diameters can be almost free from contaminations or defects, making them ballistic 1D conductors. In contrast, multiwall carbon nanotubes (MWNTs), with diameter typically one order of magnitude larger, contain a much larger density of defects and a reduced conductance. Thus, MWNTs represent interesting model systems to investigate quantum interference phenomena resulting from intrinsic disorder[2], and since a few years much effort has been devoted to understand their quantum transport properties at low temperatures.

In particular, the cylindrical topology of the MWNTs allows to explore unique conductance patterns in presence of external magnetic fields. For weakly disordered systems and coaxial magnetic fields, Altshuler-Aronov-Spivak (AAS) oscillations of the magnetoconductance (MC) with a magnetic flux period of $h/2e$, are expected from the theory of diffusive quantum transport[3], and have been indeed observed early on[4]. Such oscillations are explained by a field-modulated quantum interference between clockwise and counterclockwise backscattered electronic pathways, which encircle the cylinder. Since all such paths gain the same Aharonov-Bohm phase per revolution, the interference is modulated periodically with the magnetic flux. In perpendicular magnetic field, periodic oscillations do not occur, but the same coherent backscattering mechanism manifests itself in the phenomenon of weak localization (WL).

Additionally, a remarkable magnetic field dependence of the bandstructure of carbon nanotubes was predicted first by Ajiki and Ando[5], resulting in a h/e-periodic band-gap oscillation in a parallel magnetic field, associated to periodic splitting of the van-Hove singularities in the density of states (DoS)[6]. Recently, first indications of these bandstructure effects have been seen experimentally by means of photoluminescence[7], Coulomb blockade[8,9], and Fabry-Perot type interference[10]. In Ref. 9 a h/e-periodicity of single particle states has been

reported, but the subband spacing extracted was one order of magnitude too small.

However to date, the precise interpretation of the magnetoconductance remains an issue of debate and controversies. Indeed, while first reports of magnetotransport in MWNTs disregarded any band-structure contributions[2], others have exclusively assigned Aharonov-Bohm oscillations to gap-modulations and van-Hove singularities shifting[11]. Fujiwara and coworkers[12] further show that a switching from negative to positive magnetoresistance was possible by changing the orientation of the magnetic field from parallel to perpendicular direction with respect to the tube axis.

Unusual magnetotransport phenomena due to the co-existence of different types of Aharonov-Bohm phases were then theoretically addressed[13]. Recent experimental studies in small-diameter SWNT and MWNT[14,15] have also reported on such switching of the sign of the MC under gate voltage, but due to the very small diameter, no Aharonov-Bohm oscillations could be resolved.

In this Letter, the interplay between the different magnetic flux effects and the bandstructure and localization phenomenona is investigated by studying the MC in thick MWNTs over a wide range of Fermi level positions. In contrast to earlier works, the large diameter (29 - 35nm) allows a threading flux $\phi \sim 3\phi_0$ at magnetic fields of 16 Tesla ($\phi_0 = h/e$ the quantum flux). In addition, the transport through several several subbands is explored by virtue of a strongly coupled Al backgate electrode. The measured MC reveals clear signatures of coexisting magnetic field-dependent band structure and coherent backscattering. The h/e-periodic contribution agrees well with numerical calculations of the DoS, while the $h/2e$-contribution is clearly of AAS-type. In contrast, a perpendicular field only weakly affects the DoS, the magnetoresistance being fully dominated by the coherent backscattering.

The samples were produced by deposition of individual MWNTs on oxidized Al strips and subsequent fabrication of Au contacts ([16,17] for details). The two-terminal con-
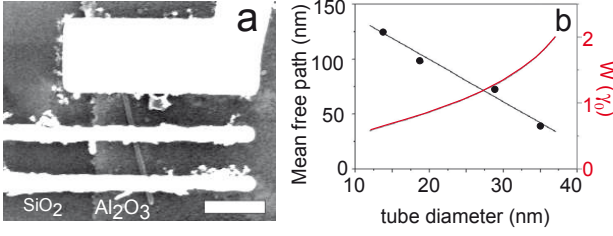
FIG. 1: a) Scanning electron micrograph of sample D. An individual MWNT is deposited on top of an oxidized Al film and contacted by three Au fingers. Only the upper two fingers are used. The scalebar corresponds to 500 nm. b) Estimate of the elastic mean free path ℓ_{el} at the CNP (black dots) and effective Anderson disorder W (red) vs. tube diameter at 10 K (see text). The black line represents a linear fit to ℓ_{el}.

ductance was measured with conventional lock-in techniques, while a dc voltage, U_{gate}, was applied to the Al backgate. Four samples, A to D, were used with diameters d_{tube} of 14, 19, 29 and 35 nm, respectively. A scanning electron micrograph of sample D is shown in Fig.1a.

The basic parameter determining the electric transport properties besides the band structure is the elastic mean free path ℓ_{el}. In carbon nanotubes, ℓ_{el} has been found to depend strongly on the position of the Fermi energy E_F[16,19], with a pronounced maximum in the vicinity of the charge neutrality point (CNP), where bonding and anti-bonding bands cross. In a conductor of length L with $N_\perp$ conducting channels per spin direction, the two terminal resistance R is given by

$$R = R_C + \frac{h}{2e^2}\left(\frac{N_\perp \ell_{el}}{L + \ell_{el}} - \frac{L_\varphi}{L}\right)^{-1}, \qquad (1)$$

where L_φ is the phase coherence length and R_C is the contact resistance and $N_\perp = 2$, at the CNP of a metallic nanotube. The position of the CNP can be identified by means of a strongly coupled Al gate and is indicated by a shallow maximum in $R(V_{gate})$ at 300 K. As in[16], the corresponding R(CNP) can be inferred. By assuming a typical value for R_C of 2.5 kΩ, a lower bound to ℓ_{el} at the CNP can be estimated from Eq. 1. The result as a function of tube diameter is presented in Fig.1b. This lower bound for ℓ_{el} decreases nearly linearly with d_{tube}, from 130 nm to 40 nm for diameters of 14 nm and 35 nm, respectively. As soon as higher nanotube subbands are occupied, Eq.1 as well as numerical results[19] predict a strong decrease of ℓ_{el} by about one order of magnitude. With the exception of a narrow region around the CNP, all of our MWNTs are thus in the diffusive regime. Only at the CNP ℓ_{el} can exceed both d_{tube} and L_φ.

In order to estimate an effective strength of the disorder potential, we use the analytical form of ℓ_{el} that has been derived for Anderson disorder with width W, i.e., $(W/\gamma_0)^2 = (18\pi/\sqrt{3}) \times (d_{tube}/\ell_{el})$, where $\gamma_0 \simeq 3$ eV is the C-C hopping matrix element[19]. The result is presented in Fig.1b (red curve). W increases with diameter
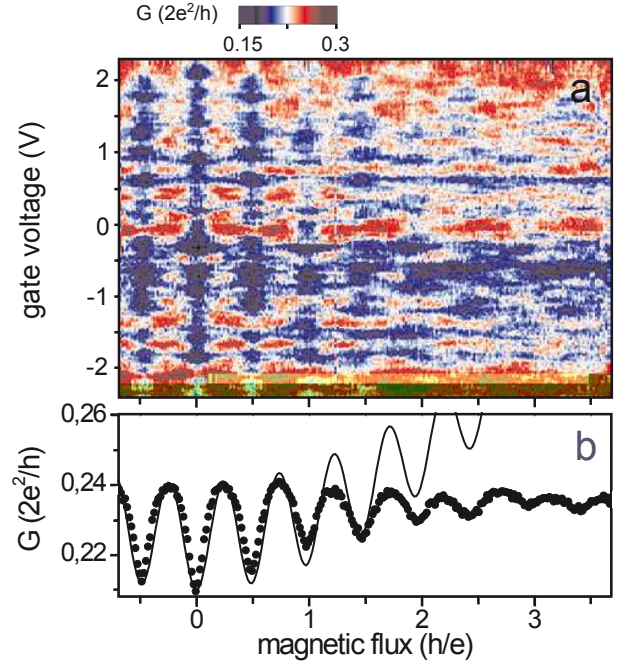

FIG. 2: a) Color representation of the differential conductance as a function of gate voltage U_{gate} and coaxial magnetic field at 4.5 K. The CNP is located in the center of the horizontal conductance valley near $U_{gate} = -0.6$ V. b) Magnetoconductance averaged over all gate voltages (dots). The line is the best fit according to the AAS-theory.

from below 1 eV to 2 eV. Thus, the disorder apparently increases with diameter for MWNTs, probably due to a larger defect density in larger diameter MWNTs, as often reported experimentally[20]. In the following, in agreement with prior studies[2,4,16], the transport is assumed to be restricted to the outermost conducting shell[18].

Next, the conductance G of samples C and D was recorded as a function of gate voltage U_{gate} and *coaxial* magnetic field B at a temperature of 4.5 K. The data for sample D are presented in Fig.2a in a color representation. The conductance is strongly modulated as a function of both magnetic field and gate voltage U_G. At our relatively high temperatures, $T \gtrsim 4.5$ K, the behavior of G is dominated by bandstructure effects and universal conductance fluctuations. For each value of the magnetic field, G is minimal in the vicinity of $U_{gate} = -0.6$ V, which can be identified with the CNP from room temperature measurements (not shown). Most MC traces show a minimum at zero magnetic field as well as at multiples of $\Delta B = 2.2$ T. ΔB agrees well with a flux period of $h/2e$, which corresponds to 2.2 T for $d_{tube} = 35$ nm. In addition, several conductance features are repeated periodically with a field period $2\Delta B$, e.g., the ridges of high conductance around zero gate voltage. Thus, two periodicities ΔB and $2\Delta B$ are superimposed, which signals the coexistence of the $h/2e$ AAS-oscillations originating from coherent backscattering and h/e Aharonov-Bohm

oscillations of the bandstructure.

If the gate voltage range is sufficiently large, an average over all MC traces removes the universal conductance fluctuations as well as the bandstructure modulations[16]. Only the contribution of the coherent backscattering to the conductance is predicted to remain[3]. The ensemble average for U_G in the interval $[-2.3$ V, 2.3 V$]$ is presented in Fig.2b. The average conductance $\langle G \rangle$ oscillates with a flux period of approximately $\simeq h/2e$ (corresponding to the outer diameter of the tube), as expected. The solid line in Fig.2b corresponds to the best fit of the AAS theory[3]. The free parameters were L_φ and the angle θ of the magnetic field with respect to the tube axis. The best agreement is obtained for $L_\varphi = 30$ nm and $\theta = 2°$. The quality of the fit is satisfactory for small fields, while for larger fields the oscillations are strongly damped and deviations in the parabolic background occur. The origin of these deviations is not clear. The flux periodicity of approximately $h/2e$ suggests that the current is carried only by few outermost shells of the MWNT. Since the periodicity reflects the average shell diameter of the transport, the inner shells apparently do not much contribute to the current.

To unravel the precise contribution of bandstructure effects from quantum interferences phenomena, a theoretical analysis of the DoS and quantum conductance in clean and disordered nanotubes is performed. First, in Fig.3a, the density of states of clean (260, 260) armchair nanotube (with diameter of 35nm) is shown as a function of the gate voltage, U_{gate}, and coaxial magnetic flux in the interval $[0, h/e]$. For the comparison of the calculated DoS to the measurement, the energy scale E has to be converted into an equivalent gate voltage scale. This has been done successfully earlier by assuming a constant capacitive coupling $C_{gate} \simeq 300$ aF/μm between the gate and the tube[16]. In a color-plot, a diamond-shaped structure is clearly visible and manifest the splitting and shift of the van-Hove singularity, driven by the magnetic field. The DoS increases from the CNP to the higher electronic subbands. Some diamonds are highlighted with dashed lines.

Figure 3b shows a close-up of the experimental data in Fig. 2a in the magnetic flux range between 0 and h/e (sample D). We find conductance ridges, which are most pronounced at intermediate flux values $\Phi = h/4e$ and $\Phi = 3h/4e$, rather than at $\Phi = 0$ and $\Phi = h/2e$ as expected from the AA-theory. The reason is the suppression of the conductance at the latter values by the AAS-effect. The latter is caused by the coherent backscattering in the disorder potential, as illustrated by the ensemble average in Fig. 2b. Taking his into account, we note are many gate voltages (e.g. 1.8, 1.3, 0.7, 0.4, 0.2, -0.3, -0.9, -1.8 V), where a conductance valley at $\Phi = h/2e$ is surrounded by conductance ridges (highlighted by dashed lines) in agreement with the AA-prediction. Although these similarities are not sufficient for a one-to-one assignment of calculation and experiment, they nevertheless demonstrate that the position, the shape, and also
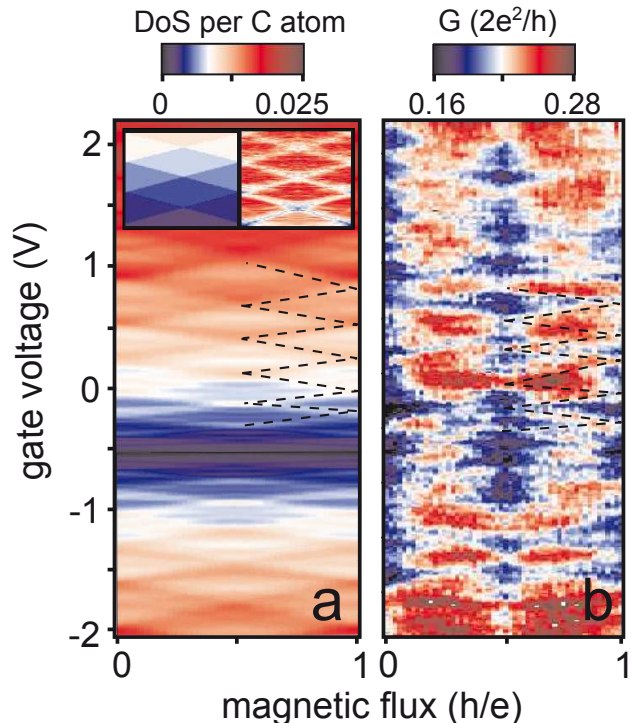

FIG. 3: a) Color representation of the calculated DoS for a (260, 260)-singlewall nanotube as a function of gate voltage and coaxial magnetic flux. The dashed lines indicate ridges of high DoS induced by the h/e-periodic splitting of van Hove singularities. Insets: Conductance of a clean (left) and disordered, $W = \gamma_0/5$, (right) (22, 22) nanotube (the x-scale is given in units of h/e, the y-scale corresponds to a small number of subbands above CNP). b) First h/e-period of the data in Fig. 2a. Dashed lines indicate diamond like ridges of high conductance.

the size of the diamonds agree reasonably well with our simple model. Similar results are obtained for sample C. In our previous experiment[16], we could link peaks in the conductance with the positions of van-Hove singularities in the DoS at the onset of the one-dimensional subbands. A very similar link between the peaks in the conductance and the DoS is reproduced by the theoretical curves in Fig. 2a.

Next, the conductance of a clean and a disordered nanotube are computed based on the Landauer-Büttiker framework[21]. Due to computational limitations, we here restrict to a (22, 22) nanotube (with 3 nm diameter), but conclusions applied equally to larger diameter owing to scaling laws. In the clean system, the ballistic conductance (Fig. 3a left inset) displays a diamond structure identical to that of the DoS (not shown here), but gives the modulation of available quantum channels under magnetic field and Fermi level shift. The conductance is constant within rhomb-shaped regions in the B-E_F-plane. At higher energy, additional conductance channels are populated, which causes a stepwise increase of
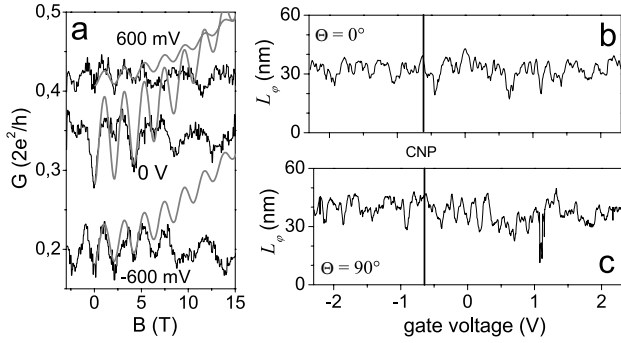
FIG. 4: a) Magnetoconductance (MC) traces at $U_{\text{gate}} = 600$ mV, 0V, -600 mV (top to bottom) (black) and fits of AAS theory (grey). Right panel: Phase coherence length vs. gate voltage for coaxial field (b) and perpendicular field (c). Vertical lines indicate the position of the CNP.

the conductance.

To explore the effect of the Anderson disorder, one can extrapolate from Fig. 1b an effective disorder strength that would correspond to an experimental measurement for a (22, 22) nanotube. The obtained value lies within $[1/10, 1/2]\gamma_0$. Using $W = \gamma_0/5$, the average quantum conductance for disordered (22, 22) nanotubes are computed (Fig. 3a right inset). The diamond shape pattern remains robust for lower energies, while it progressively degrades as higher energy subbands are involved in conduction. Therefore, the conductance increase due to the opening of channels is (over)compensated by enhanced backscattering. Calculations for much larger disorder (in the order of twice the spectral bandwith) show that such a degradation is enhanced, but rhomb-shaped regions still survive close to CNP. The estimated localization lengths are slightly smaller or of the order of the coherence length, confirming that we are in the WL regime.

After rotating the sample by 90° at low temperatures the conductance G has been recorded as a function of gate voltage and a magnetic field *perpendicular* to the tube axis. For gate voltages in the same range as for the prior case, the MC traces exhibit a minimum at $B = 0$ (not shown here), which is the negative magnetoresistance effect of the WL.[3] As expected for perpendicular magnetic fields, no field-periodic oscillations of G are observed. Instead, G is maximal at B≈2 T. For higher fields, G decreases at most gate voltages. This could be

explained in terms of bandstructure effects in perpendicular fields, where a decrease of the DoS is predicted close to the CNP[6]. Finally, in contrast to the h/e-splitting of the van-Hove singularities in coaxial field, no such effect is observed for perpendicular fields.

The relevant length scale governing the contribution of coherent backscattering to the conductance is the phase coherence length L_{φ}, which can be independently extracted from the fits of $G(B, U_{\text{gate}})$ to the WL and AAS theories, respectively. The result should be independent of the orientation of B with respect to the tube axis. Figure 4a shows some representative $G(B_{\parallel})$ traces at different U_{gate}. The fits reproduce the oscillatory part of the the experimental traces, but contain also a pronounced monotonic background, which is absent in the data. At present, the origin of this discrepancy is unclear, since this background is expected from the the small misalignment of 2° between the tube axis and the magnetic field. Nevertheless, L_{φ} can be extracted with sufficient accuracy from the amplitude of the first period of the oscillation. The result is plotted in Fig. 4b and shows pronounced variations with U_{gate}. Figure 4c shows $L_{\varphi}(U_{\text{gate}})$ extracted from the $G(B_{\perp})$-traces. The two $L_{\varphi}(U_{\text{gate}})$ curves agree well in absolute value. The correlation in the position of the minima appears to be weak. Given the superimposed effect of aperiodic conductance fluctuations (UCF) in the individual MC-traces and the systematic shift of the van-Hove singularities with magnetic field for parallel orientation this is not too surprising. Unlike in the case of samples A and B[16], the disorder in the 35 nm thick sample D seems to be too strong compared with the subband spacing, to allow an analogous identification of all subband adjacent to the CNP.

In conclusion, unambiguous signatures of magnetic-field dependent and quantum interference phenomena have been shown to jointly contribute to the magneto conductance of large diameter MWNTs. Different types of Aharonov-Bohm phases were identified, resulting in a comprehensive description of quantum transport in diffusive multiwall carbon nanotubes.

[1] C. Dekker, Physics Today **52**, 22 (1999). Ph. Avouris, MRS Bulletin, June 2004, pp. 403.

[2] C. Schönenberger, A. Bachtold, Ch. Strunk, J.-P. Salvetat, L. Forró, Appl. Phys. A **69**, 283 (1999).

[3] for a review see: A. G. Aronov and Yu .V. Sharvin, Rev. Mod. Phys. **59**, 755 (1987) and the references therein.

[4] A. Bachtold *et al.*, Nature **397**, 673 (1999).

[5] H. Ajiki, T. Ando, J. Phys. Soc. Jpn. **62**, 1255 (1993).

[6] S. Roche, D. Dresselhaus, M.S. Dresselhaus, R. Saito, Phys. Rev. B **62**, 16092 (2000).

[7] S. Zaric, *et al.*, Science **304**, 1129 (2004).

[8] P. Jarillo-Herrero *et al.*, Phys. Rev. Lett. **94**, 156802 (2005).

[9] U.C. Coscun *et al.*, Science **304**, 1132 (2004).

[10] J. Cao, Q. Wang, M. Rolandi, H.J. Dai, Phys. Rev. Lett. **93**, 216803 (2004).

[11] J.-O Lee *et al.*, Phys. Rev. B **61**, 16362 (2000); Phys. Rev. B **64**, 157402 (2001.) C. Schönenberger, A. Bachtold, Phys. Rev. B **64**, 157401 (2001).

[12] A. Fujiwara *et al.*, Phys. Rev. B **60**, 13492 (1999).

[13] S. Roche, R. Saito, Phys. Rev. Lett. **87**, 246803 (2001).

[14] G. Fedorov *et al.*, Phys. Rev. Lett. **94**, 066801 (2005).

[15] H. T. Man and A. F. Morpurgo, Phys. Rev. Lett. **95**, 026801 (2005).

[16] B. Stojetz, C. Miko, L. Forró, Ch. Strunk, Phys. Rev. Lett. **94**, 186802 (2005).

[17] B. Stojetz *et al.*, New J. Phys. **6**, 27 (2004).

[18] B. Bourlon *et al.*, Phys. Rev. Lett. **92**, 026804 (2004).

[19] C.T. White, T.N. Todorov, Nature **393**, 240 (1998). F. Triozon, S. Roche, A. Rubio, D. Mayou, Phys. Rev. B **69**, 121410 (2004).

[20] M.S. Dresselhaus, P.C. Eklund, Adv. Phys. **49**, 6 (2000).

[21] F. Triozon, Ph. Lambin, S. Roche, Nanotechnology **16**, 230 (2005).